Peer Community Journal

Section: Infections

Research article

Published 2025-11-27

Cite as

Stefania Porcelli, Delphine Le Roux, Aurélie Heckmann, Clémence Galon, Lourdes Mateos-Hernandez, Ladislav Šimo, Alejandro Cabezas-Cruz, Anne-Claire Lagrée, Grégory Karadjian, Pierre Lucien Deshuillers and Sara Moutailler (2025) Interaction dynamics of Borrelia afzelii and tick-borne encephalitis virus in C3H mice: insights into immune response, Peer Community Journal, 5: e131.

Correspondence

pierre.deshuillers@vet-alfort.fr sara.moutailler@anses.fr

Peer-review

Peer reviewed and recommended by PCI Infections,

https://doi.org/10.24072/pci. infections.100251



This article is licensed under the Creative Commons Attribution 4.0 License.

Interaction dynamics of *Borrelia afzelii* and tick-borne encephalitis virus in C3H mice: insights into immune response

Stefania Porcelli¹, Delphine Le Roux¹, Aurélie Heckmann¹, Clémence Galon¹, Lourdes Mateos-Hernandez¹, Ladislav Šimo¹, Alejandro Cabezas-Cruz¹, Anne-Claire Lagrée¹, Grégory Karadjian¹, Pierre Lucien Deshuillers¹, and Sara Moutailler¹

Volume **5** (2025), article e131

https://doi.org/10.24072/pcjournal.660

Abstract

Ticks are important vectors responsible for transmitting a wide range of diseases that have significant impacts on both human and animal health. In Europe, the *Ixodes* tick is especially remarkable for its ability to spread pathogens such as *Borrelia*, the bacterium that causes Lyme disease, and the tick-borne encephalitis virus (TBEV), which can lead to serious neurological infections. Building on the results of our previous research involving co-infection with *Borrelia afzelii* and TBEV in C3H mice, this study aimed to further investigate the interactions between these two pathogens, focusing on the timing of infection and examining mRNA cytokine levels in the brain and spleen of both single- and co-infected mice and their possible link to the clinical outcome. The results revealed that the timing of infection significantly influenced the immune response, highlighting the complex interactions between *B. afzelii* and TBEV. *B. afzelii* infection can influence TBEV dynamics, either amplifying or suppressing its effects depending on the timing of infection. In addition, this study helps to better understand how the immune system reacts when both TBEV and *B. afzelii* infect a host under different conditions. It sheds light on how these pathogens interact and affect disease progression.

¹ANSES, INRAE, Ecole Nationale Vétérinaire d'Alfort, UMR BIPAR, Laboratoire de Santé Animale, F-94700 Maisons-Alfort, France







Introduction

Ticks are a significant group of arthropod vectors, known for the wide range of pathogens they carry and their serious impact on both human and animal health (Jongejan & Uilenberg, 2004). In Europe, Ixodes ricinus stands out as the most important due to its extensive presence across various ecosystems and its ability to transmit numerous microorganisms. These include *Borrelia burgdorferi* s.l. (the bacterium responsible for Lyme disease) and the virus that causes tick-borne encephalitis (TBEV) (de la Fuente et al., 2017). Adding to the challenges posed by tick-borne diseases, is the frequent occurrence of co-infections, where a single host is infected with multiple pathogens at the same time. In Europe, tick-borne co-infections often involve combinations of pathogens such as *B. burgdorferi* s.l., *Anaplasma phagocytophilum*, and *Babesia microti* (Rocha et al., 2022). Other common pairings include *B. burgdorferi* s.l. with *A. phagocytophilum* or *A. phagocytophilum* with *Rickettsia* species (Rocha et al., 2022).

Co-infections involve not only two bacteria or a combination of a bacterium and a parasite, but can also include viruses, such as TBEV. Importantly, a significant proportion of individuals with tick-borne co-infections, such as those with TBEV and/or *B. afzelii*, experience more pronounced symptoms. However, the link between co-infection and severe clinical outcome is still unclear, as suggested by several studies (Dumic et al., 2021; Moniuszko et al., 2014; Wormser et al., 2019). The overlapping symptoms and different incubation periods of each pathogen further complicate diagnosis and testing, making it difficult to accurately identify infections. For this reason, it is crucial to understand the impact of co-infections, which requires a deeper understanding gained through advanced animal models (Porcelli et al., 2024a).

Human co-infections with TBEV and B. burgdorferi s.l. have been documented in Europe and Asia, although most reports consist of individual cases or small series in which the precise timing of infection is difficult to establish, as many diagnoses rely on serology rather than synchronous pathogen detection. In a classic Slovenian series of acute lymphocytic meningitis, patients showed laboratory evidence of concomitant TBEV and B. burgdorferi s.l. infection and frequently presented initially with typical TBE symptoms followed by Lyme manifestations during follow-up, a pattern consistent with simultaneous or closely timed acquisition from a single tick bite (Cimperman et al., 1998). Similarly, a Latvian cohort of infected patients with TBEV and B. burgdorferi s.l. described overlapping neurological presentations dominated by meningitis or meningoencephalitis, emphasizing the need to test for both pathogens following tick exposure in endemic areas (Logina et al., 2006). Individual case reports provide additional evidence of likely near-simultaneous infections. These include patients with severe meningoencephalitis who showed parallel rises in serum IgG levels against both TBEV and B. burgdorferi s.l., suggesting that both infections occurred around the same time following a single exposure (Boyer et al., 2018, 2022; Ostapchuk et al., 2023). Across studies, true concurrent clinical co-disease appears uncommon compared to serological co-exposure, and a recent systematic review concluded that many TBE patients who are Borrelia-seropositive likely represent prior exposure rather than active dual infection at presentation. Regarding disease severity, the same review found no consistent evidence that coinfected patients experience systematically worse outcomes than those with single infections, although additive clinical pictures such as erythema migrans accompanied by high fever or neuroborreliosis overlapping with confirmed TBE were observed in a subset. Finally, co-detections of TBEV and B. burgdorferi s.l. in questing I. ricinus ticks support the biological plausibility of simultaneous human exposure within a single season, providing an ecological context for the clinical observations (Boyer et al., 2022; Oechslin et al., 2017; Waiß et al., 2024).

Co-infection experiments in mouse models have shown that when mice are infected with two pathogens, their immune response is altered. This can lead to higher bacterial loads, longer persistence of infection and worse disease outcomes (Holden et al., 2005; Thomas et al., 2001; Zeidner et al., 2000). Holden's study in mice showed that co-infection with *B. burgdorferi* s.s. did not increase levels of *A. phagocytophilum* in the bloodstream, but did alter the immune response, reducing antibody levels against *A. phagocytophilum* (Holden et al., 2005). This finding is

consistent with previous research by Zeidner et al. (2000) who also found changes in cytokine profiles, suggesting that co-infections may involve immunomodulatory mechanisms (Holden et al., 2005; Zeidner et al., 2000). In addition, Thomas et al. (2001) observed that mice infected with both *B. burgdorferi* s.s. and *A. phagocytophilum* had lower levels of key immune signals such as IFN- γ , IL-12 and TNF- α , but higher levels of IL-6 compared to those infected with *B. burgdorferi* s.s. alone (Thomas et al., 2001). Moreover, macrophages from co-infected mice had reduced expression of the IFN- γ receptor, further suggesting that co-infection disrupts the immune response.

Previous work in our laboratory established co-infection models in C3H mice with *B. afzelii* and TBEV, showing that the outcome varied depending on the time of infection. Indeed, clinical signs associated with TBEV infection were more prominent in mice infected with TBEV 9 days after *B. afzelii* primo-infection compared to mice infected with TBEV 21 days after *B. afzelii* infection (Porcelli et al., 2024b).

A second experiment in mice with the same pathogens and same kinetics of TBEV and *B. afzelii* infections was performed to understand how the immune system reacts to infection and to better understand the interactions between the pathogens and the host immune system. Therefore, the present study investigated the mRNA cytokine expression levels in brain and spleen of C3H mice infected with *B. afzelii* and then TBEV 9 days or 21 days post bacterial infection or co-infected simultaneously with both pathogens and compared them to those in mice with single infections. This study participates in understanding the role of the host immune system in the interactions between *B. afzelii* and TBEV, offering insight into a situation that can realistically occur in nature and in human cases.

Materials and methods

Ethics statement

In vivo experiments were performed at the Animal Facility of the Laboratory for Animal Health of the French Agency for Food, Environmental and Occupational Health & Safety (ANSES), Maisons-Alfort, France, according to French and International Guiding Principles for Biomedical Research Involving Animals (2012). The present research was conducted in compliance with all relevant European Union guidelines for work with animals and with the French national law guidelines on the use of experimental animals and the protection of animals against cruelty. Experimental protocols were approved by the ANSES-ENVA-UPEC Ethics Committee for Animal Experimentation (Approval Numbers: APAFIS #35511-2022022111197802 v2, Date of agreement 2022/04/14; APAFIS#31496-2021051213296446 v3; Date of agreement 2021/06/18).

Mice and Housing Conditions

Six-week-old female C3H/HeN (C3H) mice were obtained from Charles River Laboratories (France). The mice were maintained in groups of six, or five for the TBEV infection group, in plastic cages with wood-chip bedding, fed ad libitum, and kept in standardized conditions (21 $^{\circ}$ C, 12-hour light/12-hour dark photoperiod) ANSES in Maisons-Alfort, France. Each mouse was identified with a subcutaneous microchip (Biolog Tiny, 1,4 × 8 mm; Biolog-Animal, France) for precise tracking throughout the study, and they were monitored twice daily to document and report any deviations from normal behavior or signs of health decline. Animal housing and handling took place under Biosafety level 3** (BSL3**) conditions.

Bacterial culture

Low passage of *B. afzelii* CB43 (Štěpánová-Tresová et al., 2000) was started from glycerol stocks and grown in Barbour-Stoenner-Kelly (BSK)-H (Sigma-Aldrich, St. Louis, MO, USA) medium with 6% rabbit serum at 33°C for 7 days after being started from glycerol stocks (Pospisilova et al., 2019). This strain (CB43) was initially isolated from one questing female *I. ricinus* collected in the Czech Republic in 1998 (Štěpánová-Tresová et al., 2000).

Viral culture

The TBEV strain Hypr (2.3x10⁶ PFU/mL) was used for animal infections. This strain was initially isolated from human blood, in Czech Republic, in 1953 (Wallner et al., 1996). In laboratory, TBEV Hypr was passaged four times in suckling mice brains and twice in Vero E6 cells, before being passaged tree times in our laboratory and used in the experiments (Yasumura & Kawakita, 1963; Migné et al., 2022).

Experimental infection of mice

After a one-week acclimatization period, 40 mice were divided into six study groups; mice infected only with B. afzelii (n = 6, called "B. afzelii"), another group infected only with TBEV (n = 10, called "TBEV") and two "super-infection" groups, where mice were first infected with B. afzelii and later exposed to TBEV, after the immune system has started responding to B. afzelii. Superinfection refers to a condition in which an organism is sequentially infected with two different pathogens, where the second infection occurs after the immune system has started responding to the first one. In the "Super-infection 21" group (n = 6, called "S21"), mice were infected with B. afzelii followed by TBEV after 21 days, whereas in the "Super-infection 9" group (n = 6, called "S9"), the second infection occurred earlier, just 9 days after the initial B. afzelii infection. Additionally, there was a co-infection group (n = 6, called "Co-inf."), in which mice were infected with both pathogens simultaneously and a negative control group (n = 6, called "Neg") where mice received BSK-H medium (Figure 1). Mice were infected with B. afzelii (Figure 1) with 1×106 spirochetes of the CB43 strain, in BSK-H medium, administered by a combination of subcutaneous (100 μL) and intraperitoneal (150 μL) injections. The subcutaneous dose was obtained by diluting a stock suspension of 20×107 spirochetes/mL 1:10 to achieve the final concentration of 1×106 spirochetes in 100 µL (Porcelli et al., 2024b; Wu-Chuang et al., 2023). In the TBEV group, mice were infected by subcutaneous injection of 100 µL of a diluted Hypr strain virus suspension containing 1×10² PFU/mouse. The inoculum was prepared by performing serial 1:10 dilutions of the original stock (2.3×10⁶ PFU/mL) in DMEM to reach a final concentration of 1×10³ PFU/mL. This applies for all groups (simply infected or super infected at 21 or 9 days) except Neg mice which received 100 µL of BSK-H medium subcutaneously. Over 14-day post-TBEV infection (p.t.i.) observation period, TBEV-specific clinical signs such as ruffled fur, hunched posture, paralysis and mortality were documented for each mouse. In case of severe clinical signs of TBEV observed, mice were euthanized before the endpoint of the study to prevent mRNA degradation. At the endpoint, brain and spleen were gathered and stored at - 80°C until further use (Figure 1).

Blood sample collection and preparation

Blood samples (50 μ L) were collected from each mouse on days 0, 5, 8, and 10 p.t.i. through retro-orbital sampling from all experimental groups in sterile tubes containing 30 μ L EDTA. The entire anticoagulated blood sample (80 μ L) was added to 350 μ L of lysis buffer (RA1) and 3.5 μ L of β -mercaptoethanol in tubes, following the NucleoSpin® RNA extract II kit instructions (Macherey Nagel, Germany). These tubes were then frozen at -80°C until RNA extraction.

RNA extraction

RNA was isolated from the entire anticoagulated blood samples (80 μ L) using the NucleoSpin® RNA extract II kit (Macherey Nagel, Germany) following the manufacturer's instructions. The eluted RNA samples (40 μ L) were stored at -80°C.

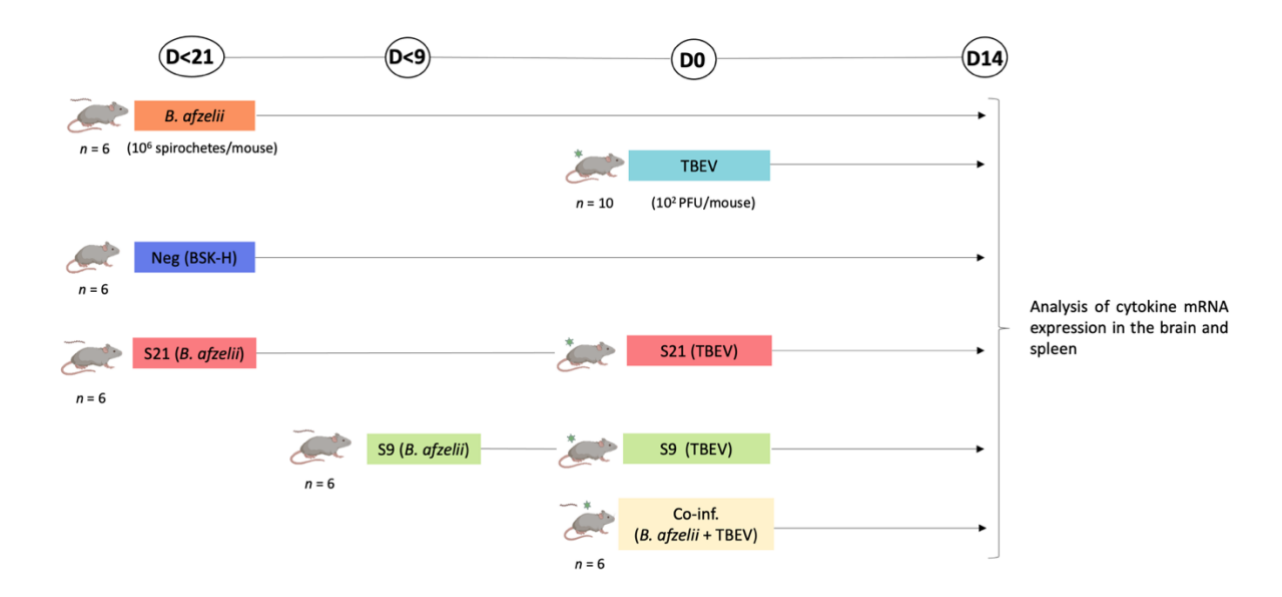


Figure 1 - Schematic representation of the experimental procedure. Infection of C3H mice at different time points. *B. afzelii*: mice infected with $1x10^6$ spirochetes of *B. afzelii*/mouse (n = 6), TBEV: mice infected with $1x10^2$ PFU/mouse (n = 10), Neg: mice inoculated with 100 μL of BSK-H medium (n = 6), S21: mice infected with *B. afzelii* followed by TBEV after day 21 (n = 6) (same doses as single infection), S9: mice infected with *B. afzelii* followed by TBEV after 9 days (n = 6) (same doses as single infection), Co-inf: mice infected simultaneously with *B. afzelii* and TBEV (n = 6) (same doses as single infection). TBEV infection was monitored by real-time RT-PCR on blood samples collected on days 0, 5, 8, and 10 p.t.i and mice still alive were sacrificed on day 14 p.t.i to collect organs (brain and spleen). Organs (brain and spleen) were tested for mRNA expression levels of inflammatory cytokines using RT-qPCR.

Real-time RT-PCR for TBEV detection in the blood and in the brain

Real-time RT-PCR was carried out on blood and brain samples utilizing the LightCycler® 480 RNA Master Hydrolysis Probes kit (Roche Diagnostics, Germany) following the manufacturer's guidelines. The real-time RT-PCR reaction volume was 20 μ L, consisting of 7.4 μ L of LightCycler® 480 RNA Master Hydrolysis Probes, 8.05 μ L of water, 1.3 μ L of activator, 2 μ L of primers and probes for detecting mRNA *B. afzelii* or RNA TBEV (Table 1), and 2 μ L of RNA template.

The real-time RT-PCR settings consisted of a reverse transcription step at 63°C for 3 min, followed by a denaturation step at 95°C for 30 seconds, 45 successive cycles at 95°C for 10 seconds, 60°C for 30 seconds, and 72°C for 1 seconds, and a final cooling step at 40°C for 30 seconds. The LightCycler® 480 Software (Roche Diagnostics, Germany) was used to acquire and analyze the data.

Species	Primer	Sequence (5' → 3')	Target Gene (Size [bp])	Reference
Borrelia afzelii	Bo_af_fla_F Bo_af_fla_R Bo_af_fla_P	GGAGCAAATCAAGATGAAGCAAT TGAGCACCCTCTTGAACAGG TGCAGCCTGAGCAGCTTGAGCTCC	Flagellin (fla) (116)	(Michelet et al., 2014)
Tick-borne encephalitis virus European subtype	TBE Euro F TBE Euro R TBE Euro P	TCCTTGAGCTTGACAAGACAG TGTTTCCATGGCAGAGCCAG TGGAACACCTTCCAACGGCTTGGCA	Envelope protein (E) (91)	(Gondard et al., 2018)

Table 1 - Oligonucleotide primers used to detect tick-borne pathogens.

RNA extraction from organs

The MagMAXTM mirVanaTM Total RNA Isolation Kit (Thermo Fisher Scientific, France) was used for mouse tissue RNA extraction. The tissues (½ brain, ½ spleen) were immersed in 1.5 mL of RNAlater solution (Thermo Fisher Scientific, France), incubated overnight at 4°C and then stored at -80°C before performing an RNA extraction. The tissue was then removed from the RNAlater solution with sterile tweezers, the excess RNAlater solution was quickly blotted off with tissue paper and the sample was then immersed in RNA Isolation Lysis Solution. To determine the amount of lysis solution required to homogenize the tissue, a ratio of 1:20 was used for brain tissue and 1:40 for spleen tissue. For the brain tissue, 1.2 g was mixed with 2 mL of lysis buffer and 14 μL of β-mercaptoethanol. For the spleen tissue, 1.7 g was mixed with 2.6 mL of lysis buffer and 18 μL of β -mercaptoethanol. Three crushing cycles (20 seconds) were performed using a six-bead stainless steel FastPrep-24™ 5G tissue homogenizer (MP Biomedicals, USA), followed by a 2minute centrifugation at 14,000 g. The resulting supernatant was vortexed and 100 µL were transferred to a separate well of a KingFisher™ 96 Deep-Well Plate. For splenic tissue, an additional 10 µL of chloroform was added to each well. The plate was then covered and shaken at 1,150 rpm for 5 minutes. Then 100 µL of isopropanol were added, and the plate was covered and shaken at 950 rpm for 2 minutes. Next, 20 µL of the prepared Binding Beads Mix were added and the plate was shaken for 5 minutes at 950 rpm.

Subsequently, the plate was washed using the KingFisher TM Flex 96 Deep-well Head Magnetic Particle Processor as follow: first, 150 μ L of Wash Solution I and then 150 μ L of Wash Solution II were added to the plate. After treating the beads with 50 μ L Turbo DNase, 50 μ L Rebinding Buffer were added to facilitate RNA binding to the beads. Then 100 μ L of isopropanol were added to precipitate the RNA. The beads with bound RNA were washed with the Wash Solution II to remove contaminants and the RNA was eluted from the beads using 100 μ L of Elution Buffer (supplied with the kit). RNA was quantified by a Nanodrop. The eluted RNA was stored at -80 °C before further use.

Cytokine expression in organs

Multiple cytokines mRNA expressions were determined with a cytokine array (Mouse Inflammatory Cytokines & Receptors RT2 Profiler PCR Array, Qiagen, France) (Arikawa et al., 2011.; Karadjian et al., 2017) accordingly to the manufacturer's instructions, first on brain pooled RNA extracts and then on spleen pooled RNA extracts from TBEV-infected mice within each infection scenario group.

In order to remove genomic DNA from pooled RNA extracts, a genomic DNA elimination mix (consisting of 2 μ L of Buffer GE, 0.5 μ g of total RNA and variable RNase free-water) was prepared for a total volume of 10 μ L. The genomic DNA elimination mix was incubated for 5 min at 42°C, then placed immediately on ice for at least 1 min. Then, the reverse transcription mix was prepared following the manufacturer's instructions. The 10 μ L reverse transcription mix were then combined with 10 μ L of the genomic DNA elimination mix and the samples were incubated at 42°C for 15 minutes followed by a 95°C incubation step for 5 minutes. The resulting cDNA was used for Real-Time PCR with the RT2 Profiler PCR Array. A total of 102 μ L of the first-strand cDNA were mixed with 1350 μ L of 2x RT2 SYBR Green qPCR Master Mix and 1248 μ L of RNase-free water.

The qPCR was performed on a LightCycler® 480 (Roche, France) according to the RT2 Profiler PCR Array instructions with the following steps: an initial step at 95°C for 10 minutes, then 40 cycles at 95°C for 15 seconds and 60°C for 1 minute and a final cooling step at 40°C for 10 seconds. Each array included five housekeeping genes (Actb, B2m, Gapdh, Gusb, Hsp90ab1) for data normalization. The microarray data were normalized against these housekeeping genes by calculating the $\Delta\Delta$ Ct for each gene of interest. Fold changes in gene expression, scatterplots, and heatmaps were analyzed and generated using the RT2 PCR Array Data Analysis Software Web Tool (https://dataanalysiS9.giagen.com/pcr).

Real-time quantitative RT-qPCR analysis of single gene expression using QuantiTect Primer Assays

Reverse Transcription

Reverse transcription was performed using the QuantiTect Reverse Transcription Kit (Qiagen, France) on all brain and spleen RNA extracts from infected and uninfected TBEV mice.

The samples contained 0.2 μ g of RNA and were treated for genomic DNA elimination according to the manufacturer's instructions prior to reverse transcription. For reverse transcription, 1 μ L of Quantiscript Reverse Transcriptase, 4 μ L of Quantiscript RT Buffer 5x and 1 μ L of RT primer mix were added to the total 14 μ L genomic DNA elimination reaction with a total volume of 20 μ L. The samples were then incubated at 42°C for 15 minutes and 95°C for 3 minutes to inactivate the Quantiscript Reverse Transcriptase. The cDNA samples were stored at -20°C until real-time qPCR.

RT-qPCR analysis

For the quantitative RT-qPCR using the QuantiNova SYBR Green PCR Kit (Qiagen, France), the following bioinformatically validated QuantiTect primers from Qiagen were used: TNFα (Mm_Tnf), IFNγ (Mm_Ifng_1_SG), IL-1a (Mm_Il1a_1_SG), IL-4 (Mm_Il4_1_SG), IL-6 (Mm_Il6_1_SG), IL-10 (Mm_Il10_1_SG), IP10/CXCL10 (Mm_Cxcl10_1_SG), CXCR3 (Mm_CXCR3_1_SG), CCL5-RANTES (Mm_Ccl5_2_SG).

The reaction mix consisted of 10 μ L of 2x QuantiNova SYBR Green PCR Master Mix, 2 μ L of 10X Quantitect Primers, 6 μ L of RNase-free water and 2 μ L of cDNA, giving a total reaction volume of 20 μ L. Mouse beta-actin was used as a housekeeping gene. The amplification protocol consisted of an initial step at 95°C for 2 minutes, followed by 45 cycles of denaturation at 95°C for 5 seconds, annealing/extension at 60°C for 10 seconds and a final cooling step at 40°C for 10 seconds using the LightCycler® 480 instrument. Quantification of gene expression was performed using the comparative $\Delta\Delta$ CT method, with results reported as fold difference relative to the housekeeping gene. To calculate the fold change, the CT of the housekeeping gene was subtracted from the CT of the target gene to obtain the Δ CT. The change in expression of the normalized target gene was expressed as 2^- $\Delta\Delta$ CT, where $\Delta\Delta$ CT = Δ CT samples - Δ CT controls, as previously described (Livak & Schmittgen, 2001).

Statistical analysis

Survival analysis was performed using the Kaplan-Meier survival curve and the log-rank Mantel-Cox test to compare differences in survival times of infected mice. Since the Shapiro-Wilk test indicated that the data did not follow a normal distribution, all subsequent analyses were conducted using non-parametric t-tests, specifically the Kruskal-Wallis test with Dunn's multiple comparisons test. Statistical analyses were performed using GraphPad Prism 10 (GraphPad Software, Inc., USA); p-values < 0.05 were considered statistically significant.

Results

This study focused on analyzing the mechanisms of the host immune response upon infections by several pathogens, which can be transmitted by ticks simultaneously or subsequently. We investigated the genes involved in immune cell recruitment and cytokine upregulation under different infection scenarios, which have been described previously and followed for this specific study (Porcelli et al., 2024b). In the described infection scenarios (Figure 1), some mice did not develop clinical signs in our TBEV and *B. afzelii* model, therefore, real-time RT-PCR was performed to identify infected mice and non-infected mice (i.e. no clinical signs observed). Then, we focused our study on the expression of 84 key inflammation-related genes on pooled brain and pooled spleen RNA extracts by RT-PCR confirmed TBEV infected mice, using the RT2 Profiler PCR array. Finally, we confirmed the microarray results analyzing selected cytokines mRNA expressions for each mouse across different infection groups.

Increased TBEV severity and mortality in S21 and S9 infection groups

Distinct clinical manifestations typical of TBEV infection, such as ruffled hair, hunched posture and paralysis (Palus et al., 2013) occurred in the TBEV, S21, S9 and co-inf. groups. Among the TBEV-infected mice in the TBEV group, eight out of ten did not show any TBEV clinical signs, while two out of ten showed all the clinical signs. In the S21 group, all six mice showed all the clinical signs of TBEV, while four out of six mice in the S9 group and three out of six mice in the co-infected group also exhibited all the clinical signs of TBEV (Table 2).

Survival was followed throughout the study, but to prevent mRNA degradation, mice were sacrificed when severe TBEV clinical signs appeared. Consequently, all mice in the negative control and B. afzelii groups, as well as those without clinical signs in the different infection groups, survived until the end of the experiment (14 days p.t.i.). Following TBEV infection, mortality rates were as follows: 100% of mice in the S21 group, 66% in the S9 group, 50% in the co-infected group and 20% in the TBEV group. Specifically, in the S21 group, all six mice died 10 days p.t.i. Mortality in the S9 group occurred between nine and 11 days p.t.i., while in the co-inf. group, three mice died between day eight and eleven p.t.i. Finally, in the TBEV group, two out of ten mice died at nine and 10 days p.t.i. Survival analysis using the log-rank Mantel-Cox test revealed significant differences between the Neg and S21 groups (p < 0.005), as well as between the Neg and S9 groups (p < 0.05) (Figure 2).

	No clinical signs	Ruffled hair	Hunched posture	Paralysis
Negative control (Neg)	6/6*	0/6	0/6	0/6
B. afzelii single infection	6/6	0/6	0/6	0/6
TBEV single infection	8/10	2/10	2/10	2/10
Super-infection 21 (S21)	0/6	6/6	6/6	6/6
Super-infection 9 (S9)	2/6	4/6	4/6	4/6
Co-infection (Co-Inf)	3/6	3/6	3/6	3/6

Table 2 - Clinical signs of C3H-infected mice with *Borrelia afzelii* and TBEV.

^{*} The ratio of mice exhibiting clinical signs/ total number of tested mice.

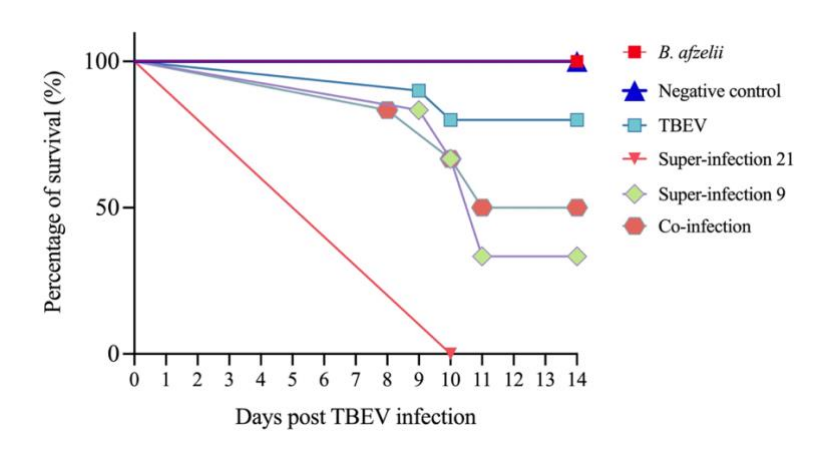


Figure 2 - Survival curve of C3H infected mice with *B. afzelii* and TBEV under different conditions. The mice were exposed to different infection scenarios. TBEV: 10^2 PFU (n = 10); *Borrelia afzelii*: 10^6 spirochetes (n = 6); S21: mice infected with *B. afzelii* followed by TBEV after 21 days (n = 6); S9: mice infected with *B. afzelii* followed by TBEV after 9 days (n = 6); Co-inf: mice infected with *B. afzelii* and TBEV simultaneously (n = 6); and one negative control group inoculated with BSK-H medium (n = 6). On day 14, all remaining mice alive were euthanized for the purpose of the study. Log-rank Mantel-Cox test revealed significant differences in survival between the Neg and S21 groups (p < 0.005), and between the Neg and S9 groups (p < 0.05).

Superinfection and co-infection lead to higher levels of TBEV RNA in the blood and brain, and the occasional detection of *B. afzelii* mRNA in the brain

To assess the presence of TBEV and *B. afzelii* in infected mice, viral RNA was detected in the blood, while both TBEV RNA and *B. afzelii* mRNA were analyzed in brain tissue.

TBEV RNA detection in the blood showed that in the TBEV group, 2/10 (20%) mice had blood infection at five and eight days p.t.i. In the S21 group, all mice had detectable TBEV RNA in the blood at five and eight days p.t.i. In the S9 group, 4/6 (66%) mice tested positive for TBEV RNA in the blood at five and eight days p.t.i. In the co-infection group, TBEV RNA was detected in the blood of 3/6 (50%) mice at five and eight days p.t.i. (Table 3). These results are consistent with TBEV-positive animals being the ones showing clinical signs of TBEV in the different infection scenarios (Table 2).

Table 3 - TBEV RNA detection in the blood of C3H-infected mice by real-time RT-PCR.

Days post TBEV infection	D0	D5	D8	D10
Negative control	0/6*	0/6	0/6	0/6
B. afzelii single infection	0/6	0/6	0/6	0/6
TBEV single infection	0/10	2/10	2/10	0/8
Super-infection 21	0/6	6/6	6/6	nd
Super-infection 9	0/6	4/6	4/6	0/2
Co-infection	0/6	3/6	3/6	0/3

^{*}The number of positive mice/number of tested mice. D=days; nd: no data.

During the 14-days observation period following TBEV infection, severe clinical signs prompted euthanasia of the mice prior to the study endpoint. This approach prevented mRNA degradation and allowed evaluation of TBEV RNA and *B. afzelii* mRNA infection in the brains of C3H mice. Table 4 shows the proportion of mice tested positive among those analyzed for brain infection under different conditions.

The detection of TBEV in the brain supported the findings in the blood: only 2/10 (20%) mice in the TBEV infection, all six mice in the S21 group, 4/6 (66%) in the S9 group and 3/6 (50%) in the co-inf. group tested positive for TBEV. In addition, *B. afzelii* mRNA was detected in two mice from the *B. afzelii* group, one mouse from the S9 group and four mice from the co-inf. group (Table 4).

Table 4 - Detection of C3H-infected mice with *Borrelia afzelii* and TBEV in the brain by Real-Time RT-PCR

	В	Brain		
	TBEV RNA	B. afzelii mRNA		
Negative control	0/6*	0/6		
B. afzelii single infection	-	2/6		
TBEV single infection	2/10	-		
Super-infection 21	6/6	0/6		
Super-infection 9	4/6	1/6		
Co-infection	3/6	4/6		

^{*}The number of positive mice/number of tested mice.

Inflammatory cytokine expression levels in brain and spleen are upregulated in superinfected and co-infected groups

Brain and spleen samples were collected from mice in each infection scenario, with six mice per group selected based on the presence of TBEV-positive blood and symptomatic manifestation, except for the TBEV group, which consisted of two infected mice. The aim was to investigate the mRNA levels of chemokines, cytokines, interleukins and their receptors involved in the inflammatory response in both brain and spleen.

For the initial cytokine analysis, brain pooled RNA extracts and then spleen pooled RNA extracts from TBEV-infected mice within each infection scenario group were used to assess the expression of 84 key genes associated with the inflammatory response, normalized to the levels of five housekeeping genes (Actb, B2m, Gapdh, Gusb, Hsp90ab1). The heat maps represent the mRNA levels of chemokines, cytokines, interleukins and their receptors involved in the inflammatory response in the RNA extracts from the brains and spleens (Figure 3A and 3B).

In the pooled RNA extracts from brains, the mice in the S21, S9, and co-infection groups had upregulated gene expression compared to the *B. afzelii* and TBEV alone infection groups. Notably, levels of mRNA CXCL-9, CXCL-10, CXCL-11, CXCL-13, IFN-γ, TNF-α, IL1-rn, CCL-2, CCL-3, CCL-4, CCL-5, CCL-7, CCL-8 and CCL-12 were upregulated (Figure 3A). Moreover, within the S21 group, mRNA levels of CXCL-1, CXCL-10, CXCL-9, CXCL-11 and CCL-12 were notably elevated compared to the S9 and co-inf. groups. Additionally, CXCL-13 mRNA levels were upregulated in the S9 group, with subsequent expression observed in the S9 and co-inf. groups. These results indicate a strong inflammatory response in the mouse brain when infected with TBEV followed by *B. afzelii* infection after 21 days.

In contrast, the level of cytokines mRNA in the pooled RNA extracts from spleens showed a lower maximum fold change (up to 14-fold) (Figure 3B) compared to the brain pooled RNA extracts, which had a maximum fold change of 1555-fold. Similarly, in the spleen pooled RNA extracts, mRNA levels of CXCL-10, CXCL-9, CXCL-11, CXCL-13, IFN-γ, TNF-α, IL-1-rn, CCL-12, CCL-2, CCL-3, CCL-4, CCL-5, CCL-7 and CCL-8 were upregulated in the S21, S9 and co-inf. groups compared to the TBEV and *B. afzelii* groups, suggesting an increase in the expression of these genes associated with a strong inflammatory or immune response to TBEV and *B. afzelii* infection (Figure 3B).

To confirm the previous results obtained during the examination of 84 key genes involved in the inflammatory response first on pooled TBEV-infected brain and then on spleen samples RNA extracts, an analysis of selected cytokines mRNA expression was performed for each mouse across different infection groups. In Figures 4 and 5, the mRNA expression levels of various cytokines in the brain and spleen of the mice have been categorized according to the severity of their clinical signs per group (severe and with no clinical signs). Based on the microarray results of the brain, and to compare the results with those reported in the literature, the mRNA levels of a broad range of cytokines (TNF-α, IFN-y, IL-1α, IL-10), the chemokine CCL-5 (RANTES), the interferon-y inducible protein-10 (IP-10/CXCL-10) and its receptor CXCR3 were quantified in the brain of C3H mice by RT-qPCR and normalized to the levels of the housekeeping gene beta-actin mRNA. The dynamics of changes in cytokine/chemokine mRNA expression were investigated between eight and eleven days p.t.i., corresponding to the time of death of the mice. The results showed an upregulation of mRNA levels for IL-10, CXCL-10, CXCR3, CCL-5 (RANTES), TNF-α, IFN-y and IL-1α in the S21, S9 and co-infection groups compared to the *B. afzelii* and TBEV groups in mice with severe clinical signs. Specifically, for IL-10 (Figure 4A), mRNA exhibited significantly upregulated expression in mice with severe clinical signs, with the highest expression observed in the S21 group, followed by the S9 group. CXCL-10 (Figure 4B) and IFN-y (Figure 4F) mRNA levels were significantly elevated in the brains of mice with severe clinical signs in the S9 and in the S21 groups, respectively. These fold changes were ten times higher than the mRNA levels of IL-10, CCL-5, TNF-α and IL-1α observed in the same groups. In addition, mRNA levels of the CXCL-10 receptor CXCR3 (Figure 4C) were upregulated in mice with severe clinical signs in the S9, S21, TBEV and co-inf. groups. Similar observations were noted for CCL-5 (Figure 4D) and TNF-α (Figure 4E) mRNA levels. Specifically, mice with severe clinical signs in the S21, S9 and co-inf. groups had higher levels of CCL-5 mRNA than those in the TBEV, B. afzelii and negative groups. Mice with severe clinical signs in the S9, S21 and co-inf. groups showed higher levels of TNF-α compared with those in the TBEV, B. afzelii and negative groups. Furthermore, elevated IL-1a mRNA levels (Figure 4G) were observed in mice with severe clinical signs in the S9, co-inf. and S21 groups, whereas lower levels were observed in mice with severe clinical signs in the TBEV group. However, IL-1α mRNA (Figure 4G) levels in mice infected with B. afzelii were higher than levels in mice with severe clinical signs in the TBEV group. Interestingly, the increase in CXCL10

and IFN-γ mRNA levels correlated with the severity of clinical signs and mortality in TBEV-infected mice from the S21 and S9 groups (Figure 2, Table 2).

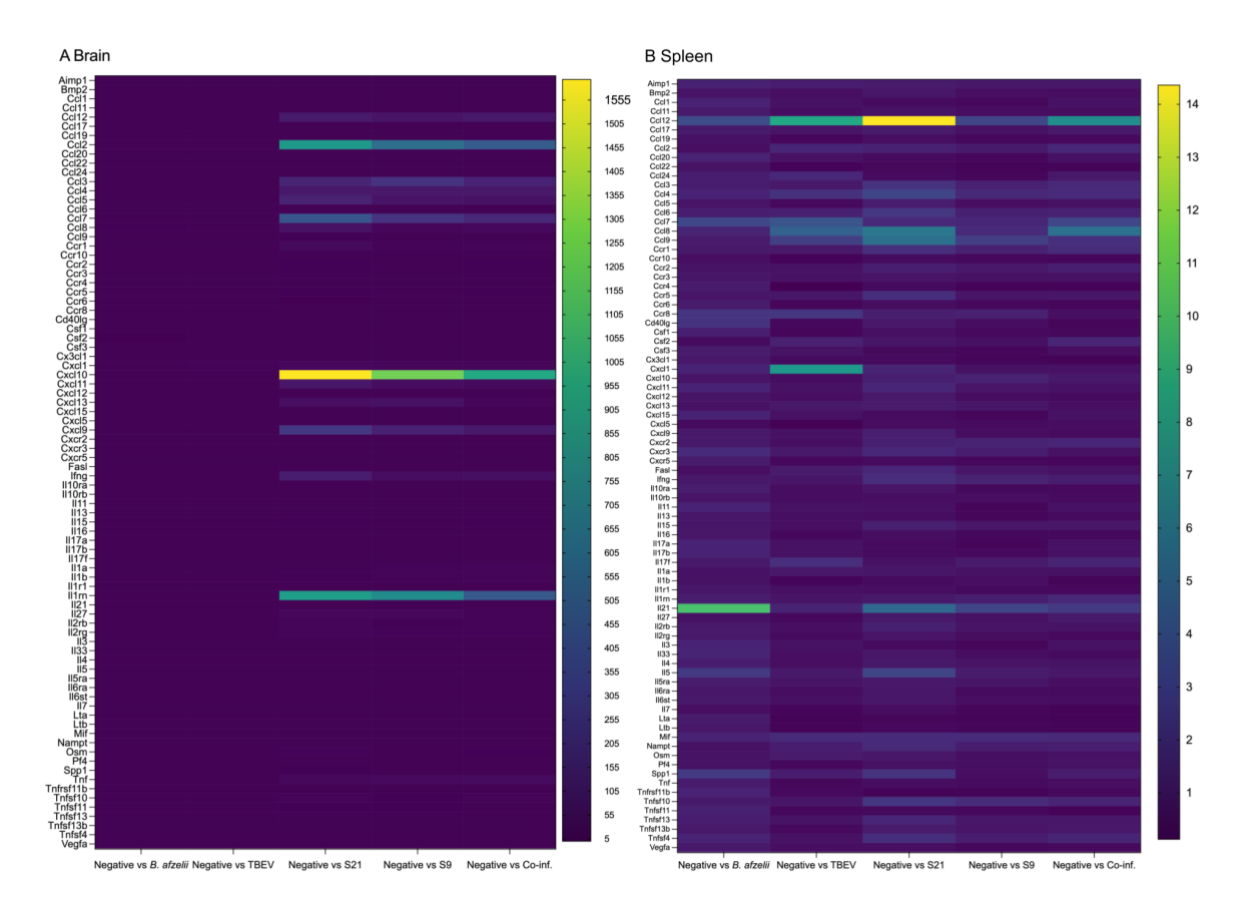


Figure 3 - Heat map analysis of cytokines mRNA levels in brain (panel A) and spleen (panel B) samples. The heat maps illustrate the differential expression levels of 84 key genes mediating the inflammatory response in TBEV-infected brain and spleen samples, including chemokines, cytokines, interleukins and their receptors. The quantification of the cytokine mRNA in the various infection groups is expressed in fold change compared to the levels of cytokine mRNA found in the Neg. group (no infection).

Similarly, to confirm the microarray results in the spleen and to compare the results with those reported in the literature, the mRNA expression levels of a wide range of cytokines (TNF-α, IFN-y, IL-4, IL-6, and IL-10), as well as interferon-y inducible protein-10 (IP-10/CXCL-10), were quantified in the spleens of C3H mice using RT-qPCR and normalized to the levels of the housekeeping gene beta-actin mRNA. The dynamics of changes in cytokine/chemokine mRNA expression were investigated between eight- and eleven-days post-infection, corresponding to the time of death of the mice. Although the fold changes in the spleen were lower than fold changes in the brain samples, the level of CXCL-10 (Figure 5F) mRNA was highest in mice with severe clinical signs in the S9 group. Similarly, IFN-y (Figure 5E) mRNA levels were higher in mice with severe clinical signs in the S9, co-infection and S21 groups. In addition, TNF-α mRNA levels (Figure 5D) were upregulated in mice with severe clinical signs in the S9 and co-infection groups. In contrast, IL-10 (Figure 5A) mRNA levels were higher in the TBEV, S21, S9 and co-inf. groups of mice with severe clinical signs. An interesting finding was the IL-4 mRNA (Figure 5C) in the B. afzelii group, which was the only cytokine to show higher levels, compared to IL-10, IL-6, TNF-α, IFN-γ and CXCL-10 in the B. afzelii group. This increase in IL-4 mRNA is consistent with the Th2 profile characteristic of extracellular bacterial infections. However, IL-4 mRNA levels were also upregulated in the S9 and co-inf. groups of mice with severe clinical signs. For IL-6 mRNA (Figure 5B), levels were

highest in the co-inf. group of mice with severe clinical signs, followed by the S21, TBEV and S9 groups.

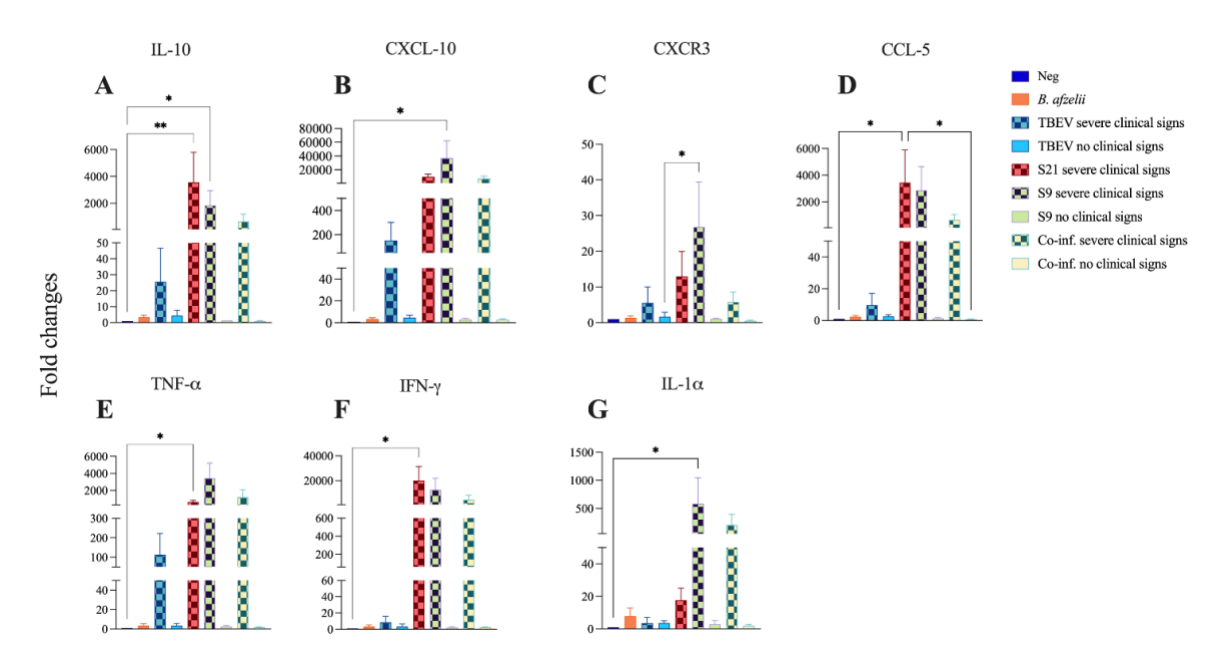


Figure 4 - Cytokines and chemokines levels were quantified in the brain of C3H mice co-infected with *B. afzelii* and TBEV under different conditions. Neg: n = 6; *B. afzelii*: n = 6; TBEV severe clinical signs: n = 2; TBEV no severe clinical signs n = 8; S21 severe clinical signs: n = 6; S9 severe clinical signs n = 4; S9 no severe clinical signs n = 2; Co-inf. severe clinical signs: n = 3; Co-inf. no severe clinical signs: n = 3. IL-10 (A), CXCL-10 (B), CXCR3 (C), CCL-5 (D), TNF-α (E), IFN-γ (F) and IL-1α (G) mRNA levels were quantified by real-time RT-qPCR and normalized to the mRNA levels of the housekeeping gene beta-actin. Of note, in the S21 group, all mice were TBEV-positive with severe clinical signs, hence the absence of a «S21 with no clinical signs» group on the graphs. Data are presented as mean ± standard deviation of fold change in mRNA levels compared to uninfected control mice. Kruskal- Wallis test with Dunn's multiple comparisons test *p < 0.05.

Discussion

In our study using co-infection models of TBEV and *B. afzelii* in C3H mice, the immune responses induced by both pathogens were investigated, and disease severity worsened when TBEV followed *B. afzelii* infection. In nature, TBEV is transmitted almost immediately during the tick bite through the saliva of infected *I. ricinus*, whereas *B. afzelii* requires a much longer feeding period, typically 24 to 48 hours, before transmission occurs (Cook, 2014; Labuda et al., 1993). The different timing of infection in our design reflects these dynamics, reproducing realistic exposure scenarios observed in the field.

Analysis of mRNA profiles revealed increased CXCL-10, IFN- γ and other cytokines mRNA levels in the brain, indicating a robust inflammation. In the spleen, IFN- γ mRNA was upregulated in severe clinical sign groups, while IL-4 mRNA levels increased in response to *B. afzelii* infection. Building on our previous established co-infection models with TBEV and *B. afzelii* (Porcelli et al., 2024b) the experiment was repeated to examine immune responses to both pathogens in C3H mice, which can co-exist in humans after a tick bite (Boyer et al., 2018; Moniuszko et al., 2014). To address age-related susceptibility, TBEV single-infection mice were increased to 10 to ensure sufficient disease for reliable comparisons; in our previous experiment, two of five 8-week-old C3H mice remained negative in the TBEV single infection, suggesting lower susceptibility at this age (Porcelli et al., 2023; Porcelli et al., 2024b).

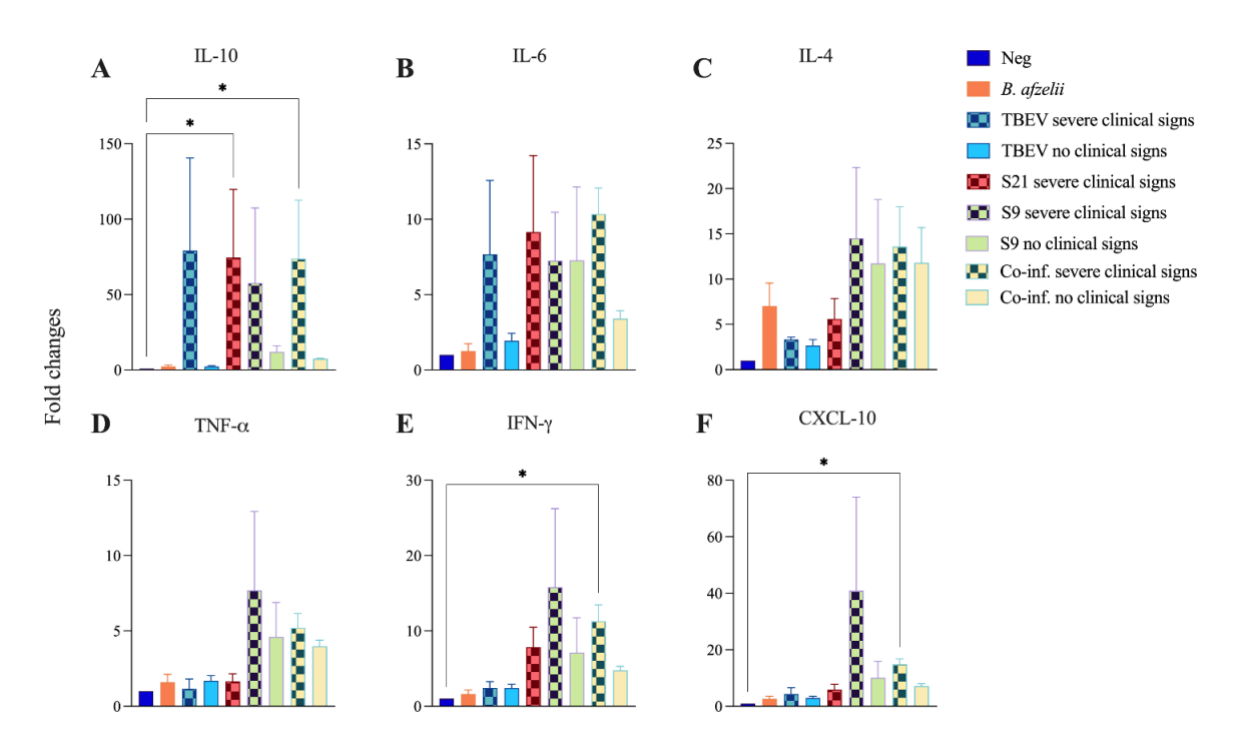


Figure 5 - Cytokines and chemokines levels were quantified in the spleen of C3H mice co-infected with *B. afzelii* and TBEV under different conditions. Neg: n = 6; *B. afzelii*: n = 6; TBEV severe clinical signs: n = 2; TBEV no severe clinical signs n = 8; S21 severe clinical signs: n = 6; S9 severe clinical signs n = 4; S9 no severe clinical signs n = 2; Co-inf. severe clinical signs: n = 3; Co-inf. no severe clinical signs: n = 3. IL-10 (A), IL-6 (B), IL-4 (C), TNF- α (D), IFN- γ (E) and CXCL-10 (F) mRNA levels were quantified by real-time RT and normalized to the mRNA levels of the housekeeping gene beta-actin. Of note, in the S21 group, all mice were TBEV-positive with severe clinical signs, hence the absence of a «S21 with no clinical signs» group on the graphs. Data are presented as mean \pm standard deviation of fold change in mRNA levels compared to uninfected control mice. Kruskal-Wallis test with Dunn's multiple comparisons test *p < 0.05, * $^*p < 0.005$.

In particular, the mechanisms of the immune were analyzed through genes involved in cell recruitment and cytokine regulation across infection scenarios.

The spleen is one of the major organs of peripheral immunity, and the central nervous system (CNS) is the main target of TBEV, B. *burgdorferi* s.s. and *B. garinii* (Casselli et al., 2021; Rupprecht et al., 2008; Růžek et al., 2011). Therefore, identifying immune response-related genes associated with TBEV and *B. afzelii* in the spleen and brain of infected mice may help us understand the immune mechanisms involved in their pathogenesis. To this end, the mRNA expression profiles of 84 key genes were analyzed in bulk and confirmed in each TBEV-positive mouse by RT-qPCR for selected genes that emerged as interesting from the heatmaps.

Consistent with prior work (Porcelli et al., 2024b), co-infection timing was critical: TBEV at 21 or 9 days after *B. afzelii* worsened clinical signs, correlating with strong inflammation marked by high IFN-γ and IL-10 in S21 and S9 groups. A high IFN-γ response in severe cases was expected but contrasts with some bacterial co-infections where IFN-γ is lower (Thomas et al., 2001; Zeidner et al., 2000). Parallel IL-10 upregulation likely reflects a feedback loop limiting damage during acute infection but potentially impairing clearance when persistent, as seen in *Toxoplasma gondii*, influenza, HIV, hepatitis B, and *Leishmania*; here, the IFN-γ/IL-10 surge suggests a balance between viral control and avoiding cytokine storm (Carlini et al., 2023), similar to patterns in *Plasmodium yoelii* with elevated IFN-γ, TNF-α, and IL-10 (Karadjian et al., 2014).

Fewer deaths were observed in the co-inf. group infected simultaneously, but recovery could not be assessed at the end of the experiment, since they were euthanized when severe clinical signs occurred, to prevent mRNA degradation. As hypothesized (Porcelli et al., 2024b), eight-week

age may influence TBEV kinetics, since only two of ten TBEV mice developed severe signs (Clark et al., 2012) aligning with evidence that age shapes antiviral immunity and disease severity (Brien et al., 2009; Clark et al., 2012; Hirsch et al., 1970; Jackson et al., 2017). For example, juvenile mice are highly susceptible to neurotropic flaviviruses such as Japanese encephalitis virus and TBEV due to immature neurons, while older mice (>18 months) also show heightened risk. Adults mice, on the other hand, typically need higher doses, reflecting receptor expression and extra-CNS replication increasing viremia and neuroinvasion (Prandovszky et al., 2008).

In addition, beyond age, prior *B. afzelii* infection (S21, S9) may alter responses to subsequent TBEV, exacerbating severity, as CNS cytokine and chemokine accumulation may accentuate progression of TBEV-related encephalitis instead of restricting viral replication (Bardina & Lim, 2012; Biswas et al., 2010; Palus et al., 2013; Shirato et al., 2004).

As observed, co-infections can worsen disease (Krause et al., 1996) through enhancement or suppression between pathogens (Homer et al., 2000). Here, *B. afzelii* followed by TBEV at days 21 and 9, or concurrently exacerbated the clinical signs of TBEV, with elevated pro- and anti-inflammatory mediators in brain linked to tissue damage and mortality; synergy likely in S21/S9 and antagonism in co-inf., consistent with documented interactions (Beaty et al., 1983; Kent et al., 2010; Moro et al., 2002; Muturi & Bara, 2015, Pesko & Mores, 2009).

In the mRNA profiling arrays, CXCL-9, CXCL-10, CXCL-11, CXCL-13, IFN-γ, TNF-α, IL1α, and CCL-2, CCL-3, CCL-4, CCL-5, CCL-7, CCL-8 and CCL-12 chemokines were upregulated in brains of S21, S9, and co-inf. mice, indicating strong inflammation. CXCL10 and IFN-γ were prominently increased, especially with severe signs, matching Pokorna Formanova et al., (2019) showing CXCL10 escalation during TBEV neuroinvasion. Although kinetics were not measured, this pattern was evident at endpoint; excessive CNS CXCL10 can be harmful (Palus et al., 2013; Sasseville et al., 1996; Sui et al., 2006) via cytotoxic T-cell recruitment and neuronal toxicity (Marle et al., 2004), and is elevated in human TBE cerebrospinal fluid (CSF). Given co-infection, *B. afzelii* brain colonization cannot be excluded despite few positive detections (Table 4); *B. burgdorferi* s.s. can colonize brain (Greenmyer et al., 2018), though mechanisms of neuroinflammation remain unclear.

Subsequently, IL-1 α and CXCL13 mRNA levels were examined as potential LNB biomarkers, given LNB manifestations and emerging CSF diagnostics (Hytönen et al., 2008; Hytönen et al., 2014; Pícha et al., 2016). In Pietikäinen, CXCL13 and IL-1 α best tracked treatment response in LNB co-infected with TBE (Pietikäinen et al., 2016). Interestingly here, IL-1 α was highest in S9, then co-inf., S21, and *B. afzelii*. Of note, the active form of IL-1 α , known as IL-1 α can induce CXCL13 production via IL1-RI receptor and NF- α B, also promoting IL-6 and TNF- α , both upregulated. Additionally, CXCL13 mRNA expression was highest in S9, then S21 and co-inf. groups; Another possible activation pathway is through TLR4 signaling. A recent study by Akoolo et al., found that TLR2/TLR4 signaling can drive inflammation even in the absence of the usual TLR4-specific LPS from *B. burgdorferi* (Akoolo et al., 2021).

Interestingly, CXCL10 and CXCR3 mRNA were significantly upregulated in severe groups (S21, S9, co-inf.), implicating them in neuroinflammation during TBEV and *B. afzelii*; parallels in West Nile Virus (WNV) show neuron-derived CXCL10 and CXCR3-linked T-cell recruitment (Lim and Murphy, 2011; Shrestha et al., 2006) which can also damage tissue (Zhang et al., 2008). Concurrently, C3H mice also showed elevated mRNA levels of CCL5-RANTES, recruiting diverse immune cells and potentially contributing to brain damage in TBE (Zhang et al., 2016; Zheng et al., 2018); with CXCL10, these mediators facilitate neuronal injury (Pokorna Formanova et al., 2019). Spatial transcriptomics of brain could localize inflammatory foci and link cellular interactions to severe outcomes.

Given the roles of CXCL10 across diseases, including vitiligo and mycoplasma infections, it is important to investigate its contribution to the pathogenesis of co-infection (Aulakh et al., 2024; Zou et al., 2025). One approach that could be tested is the modulation of the IFN-γ/CXCL10 axis using JAK/STAT1 inhibitors or CXCR3 antagonists. Ruxolitinib has been shown to reduce serum levels of CXCL10 and provide clinical benefits in the treatment of vitiligo (Passeron et al., 2024).

In the spleen, IFN-γ mRNA was upregulated only in mice with severe signs in S21, S9, and co-inf., not in severe TBEV or *B. afzelii* alone. IL-4 mRNA levels were upregulated in severe S9, co-

inf., and *B. afzelii* versus TBEV and S21, echoing tick-transmitted *B. burgdorferi* s.s.- *A. phagocytophilum* co-infection that suppressed IL-2/IFN-γ and promoted splenic IL-4 (Zeidner et al., 1997). In addition, mRNA levels of IL-6, which can bias toward Th2 (Diehl et al., 2000; Rincón et al., 1997), were upregulated in the S21, S9, co-inf. and TBEV groups in mice with severe clinical signs.

In conclusion, tackling the complexities of tick-borne diseases requires a well-rounded approach to their study, diagnosis, and treatment. By deepening our knowledge of tick-borne diseases and the dynamics of co-infections, this study adds valuable insight into how pathogens interact with their hosts and stresses the need for further research in both ticks and their animal hosts.

Funding

Authors' Contributions: Conceptualization PLD, GK, ACL, DLR, SM; methodology CG, AH, LMH, SP, and LS; formal analysis GK, DLR, SP; writing-original draft preparation PLD, GK, DLR, SM and SP; writing-review and editing, ACC, PLD, CG, AH, GK, ACL, DLR, LMH, SM, SP and LS; supervision PLD, GK, ACL, DLR and SM; funding acquisition, ACC, PLD, ACL, SM, and LS. All authors have read and agreed to the published version of the manuscript.

Research by ACC, PLD, CG, AH, GK, ACL, DLR, LMH, SM, SP and LS was supported by the French Agency for Food, Environmental and Occupational Health & Safety (ANSES), the French National Institute for Agricultural Research (INRAE), and the Ecole nationale vétérinaire d'Alfort (EnvA). UMR BIPAR is supported by the French Government's Investissement d'Avenir program, Laboratoire d'Excellence "Integrative Biology of Emerging Infectious Diseases" (grant No. ANR-10-LABEX-62-IBEID).

Declaration of competing interests

The authors declare that they comply with the PCI rule of having no financial conflicts of interest related to the content of this article.

Data, scripts, code, and supplementary information availability

The datasets generated and/or analyzed during the current study are available in the Zenodo repository (https://doi.org/10.5281/zenodo.16568808; Porcelli et al., 2025).

Acknowledgements

We thank the technical staff of the Animal Facility of ANSES for their assistance with animal care and experimental procedures. We are also grateful to colleagues from UMR BIPAR for their helpful discussions.

Preprint version 5 of this article has been peer-reviewed and recommended by PCI Infections (https://doi.org/10.24072/pci.infections.100251; Duron, 2025).

References

Akoolo, L., Djokic, V., Rocha, S. C., & Parveen, N. (2021). Pathogenesis of *Borrelia burgdorferi* and *Babesia microti* in TLR4-Competent and TLR4-dysfunctional C3H mice. *Cellular Microbiology*, **23**(9). https://doi.org/10.1111/CMI.13350

Arikawa, E., Quellhorst, G., Han, Y., Pan, H., & Yang, J. (2011). RT2 Profiler™ PCR Arrays: Pathway-Focused Gene Expression Profiling with qRT-PCR. *BioTechniques*, **43**(5)

Aulakh, S., Goel, S., Kaur, L., Gulati, S., Kaur, M., Chopra, D., Sarangal, R., & Batra, J. (2024). Differential expression of serum CXCL9 and CXCL10 levels in vitiligo patients and their

correlation with disease severity and stability: A cross-sectional study. *Indian Journal of Dermatology, Venereology and Leprology*, **91**, 9–15. https://doi.org/10.25259/IJDVL 793 2023

- Bardina, S. V., & Lim, J. K. (2012). The role of chemokines in the pathogenesis of neurotropic flaviviruses. *Immunologic Research*, **54**(1–3), 121–132. https://doi.org/10.1007/S12026-012-8333-3
- Beaty, B. J., Bishop, D. H. L., Gay, M., & Fuller, F. (1983). Interference between bunyaviruses in *Aedes triseriatus* mosquitoes. *Virology*, **127**(1), 83–90. https://doi.org/10.1016/0042-6822(83)90373-2
- Biswas, S. M., Kar, S., Singh, R., Chakraborty, D., Vipat, V., Raut, C. G., Mishra, A. C., Gore, M. M., & Ghosh, D. (2010). Immunomodulatory cytokines determine the outcome of Japanese encephalitis virus infection in mice. *Journal of Medical Virology*, **82**(2), 304–310. https://doi.org/10.1002/JMV.21688
- Boyer, P. H., Kieffer, P., de Martino, S. J., Zilliox, L., Vogel, J. Y., Jaulhac, B., & Hansmann, Y. (2018). *Borrelia burgdorferi* sl and tick-borne encephalitis virus coinfection in Eastern France. *Medecine et Maladies Infectieuses*, **48**(3), 218–220. https://doi.org/10.1016/J.MEDMAL.2017.10.006
- Boyer, P. H., Lenormand, C., Jaulhac, B., & Talagrand-Reboul, E. (2022). Human Co-Infections between *Borrelia burgdorferi* s.l. And Other *Ixodes*-Borne Microorganisms: A Systematic Review. *Pathogens (Basel, Switzerland)*, **11**(3). https://doi.org/10.3390/pathogens11030282
- Brien, J. D., Uhrlaub, J. L., Hirsch, A., Wiley, C. A., & Nikolich-Žugich, J. (2009). Key role of T cell defects in age-related vulnerability to West Nile virus. *Journal of Experimental Medicine*, **206**(12), 2735–2745. https://doi.org/10.1084/jem.20090222
- Carlini, V., Noonan, D. M., Abdalalem, E., Goletti, D., Sansone, C., Calabrone, L., & Albini, A. (2023). The multifaceted nature of IL-10: Regulation, role in immunological homeostasis and its relevance to cancer, COVID-19 and post-COVID conditions. *Frontiers in Immunology*, **14**. https://doi.org/10.3389/fimmu.2023.1161067
- Casselli, T., Divan, A., Vomhof-DeKrey, E. E., Tourand, Y., Pecoraro, H. L., & Brissette, C. A. (2021). A murine model of Lyme disease demonstrates that *Borrelia burgdorferi* colonizes the dura mater and induces inflammation in the central nervous system. *PLoS Pathogens*, **17**(2), e1009256. https://doi.org/10.1371/journal.ppat.1009256
- Cimperman, J., Maraspin, V., Lotrič-Furlan, S., Ružić-Sabljić, E., Avšič-Županc, T., Picken, R. N., & Strle, F. (1998). Concomitant infection with tick-borne encephalitis virus and *Borrelia burgdorferi* sensu lato in patients with acute meningitis or meningoencephalitis. *Infection*, **26**(3), 160–164. https://doi.org/10.1007/BF02771842
- Clark, D. C., Brault, A. C., & Hunsperger, E. (2012). The contribution of rodent models to the pathological assessment of flaviviral infections of the central nervous system. *Archives of Virology*, **157**(8), 1423–1440. https://doi.org/10.1007/s00705-012-1337-4
- Cook, M. J. (2014). Lyme borreliosis: A review of data on transmission time after tick attachment. *International Journal of General Medicine*, **8**, 1–8. https://doi.org/10.2147/IJGM.S73791
- Diehl, S., Anguita, J., Hoffmeyer, A., Zapton, T., Ihle, J. N., Fikrig, E., & Rincón, M. (2000). Inhibition of Th1 Differentiation by IL-6 Is Mediated by SOCS1. Immunity, 13(6), 805–815. https://doi.org/10.1016/S1074-7613(00)00078-9
- Dumic, I., Glomski, B., Patel, J., Nordin, T., Nordstrom, C. W., Sprecher, L. J., Niendorf, E., Singh, A., Simeunovic, K., Subramanian, A., Igandan, O., & Vitorovic, D. (2021). 'Double Trouble': Severe Meningoencephalitis Due to *Borrelia burgdorferi* and Powassan Virus Co-Infection Successfully Treated with Intravenous Immunoglobulin. *The American Journal of Case Reports*, 22(1), 1–6. https://doi.org/10.12659/AJCR.929952
- Duron, O. (2025) Modulation of the host immune response in tick-borne pathogen coinfections. Peer Community in Infections, 100251. https://doi.org/10.24072/pci.infections.100251
- de la Fuente, J., Antunes, S., Bonnet, S., Cabezas-Cruz, A., Domingos, A. G., Estrada-Peña, A., Johnson, N., Kocan, K. M., Mansfield, K. L., Nijhof, A. M., Papa, A., Rudenko, N., Villar, M., Alberdi, P., Torina, A., Ayllón, N., Vancova, M., Golovchenko, M., Grubhoffer, L., ... Rego, R.

O. M. (2017). Tick-Pathogen Interactions and Vector Competence: Identification of Molecular Drivers for Tick-Borne Diseases. *Frontiers in Cellular and Infection Microbiology*, **7**(APR). https://doi.org/10.3389/fcimb.2017.00114

- Gondard, M., Michelet, L., Nisavanh, A., Devillers, E., Delannoy, S., Fach, P., Aspan, A., Ullman, K., Chirico, J., Hoffmann, B., Van Der Wal, F. J., De Koeijer, A., Van Solt-Smits, C., Jahfari, S., Sprong, H., Mansfield, K. L., Fooks, A. R., Klitgaard, K., Bødker, R., & Moutailler, S. (2018). Prevalence of tick-borne viruses in *Ixodes ricinus* assessed by high-throughput real-time PCR. *Pathogens and Disease*, **76**(8), 1–13. https://doi.org/10.1093/femspd/fty083
- Greenmyer J.R., Gaultney R.A., Brissette C.A., Watt J.A. Primary Human Microglia Are Phagocytically Active and Respond to *Borrelia burgdorferi* With Upregulation of Chemokines and Cytokines. Front *Microbiol*. 2018 Apr 25;**9**:811. doi: 10.3389/fmicb.2018.00811.
- Hirsch, M. S., Zisman, B., & Allison, A. C. (1970). Macrophages and age-dependent resistance to Herpes simplex virus in mice. Journal of Immunology (Baltimore, Md.: 1950), **104**(5), 1160–1165. https://doi.org/10.4049/jimmunol.104.5.1160
- Holden, K., Hodzic, E., Feng, S., Freet, K. J., Lefebvre, R. B., & Barthold, S. W. (2005). Coinfection with *Anaplasma phagocytophilum* Alters *Borrelia burgdorferi* Population Distribution in C3H/HeN Mice. *Infection and Immunity*, **73**(6), 3440–3444. https://doi.org/10.1128/IAI.73.6.3440-3444.2005
- Homer, M. J., Bruinsma, E. S., Lodes, M. J., Moro, M. H., Telford, S., Krause, P. J., Reynolds, L. D., Mohamath, R., Benson, D. R., Houghton, R. L., Reed, S. G., & Persing, D. H. (2000). A Polymorphic Multigene Family Encoding an Immunodominant Protein from *Babesia microti. Journal of Clinical Microbiology*, **38**(1), 362–368. https://doi.org/10.1128/jcm.38.1.362-368.2000
- Hytönen, J., Hartiala, P., Oksi, J., & Viljanen, M. K. (2008). Borreliosis: Recent research, diagnosis, and management. *Scandinavian Journal of Rheumatology*, **37**(3), 161–172. https://doi.org/10.1080/03009740801978897
- Hytönen, J., Kortela, E., Waris, M., Puustinen, J., Salo, J., & Oksi, J. (2014). CXCL13 and neopterin concentrations in cerebrospinal fluid of patients with Lyme neuroborreliosis and other diseases that cause neuroinflammation. *Journal of Neuroinflammation*, **11**, 1–11. https://doi.org/10.1186/1742-2094-11-103
- Jackson, S. J., Andrews, N., Ball, D., Bellantuono, I., Gray, J., Hachoumi, L., Holmes, A., Latcham, J., Petrie, A., Potter, P., Rice, A., Ritchie, A., Stewart, M., Strepka, C., Yeoman, M., & Chapman, K. (2017). Does age matter? The impact of rodent age on study outcomes. Laboratory Animals, 51(2), 160–169. https://doi.org/10.1177/0023677216653984
- Jongejan, F., & Uilenberg, G. (2004). The global importance of ticks. Parasitology, **129**(S1), S3–S14. https://doi.org/10.1017/S0031182004005967
- Karadjian, G., Berrebi, D., Dogna, N., Vallarino-Lhermitte, N., Bain, O., Landau, I., & Martin, C. (2014). Co-infection restrains Litomosoides sigmodontis filarial load and plasmodial *P. yoelii* but not *P. chabaudi* parasitaemia in mice. *Parasite*, **21**, 16. https://doi.org/10.1051/parasite/2014017
- Karadjian, G., Fercoq, F., Pionnier, N., Vallarino-Lhermitte, N., Lefoulon, E., Nieguitsila, A., Specht, S., Carlin, L. M., & Martin, C. (2017). Migratory phase of *Litomosoides sigmodontis* filarial infective larvae is associated with pathology and transient increase of S100A9 expressing neutrophils in the lung. *PLoS Neglected Tropical Diseases*, **11**(5), e0005596. https://doi.org/10.1371/journal.pntd.0005596
- Kent, R. J., Crabtree, M. B., & Miller, B. R. (2010). Transmission of West Nile Virus by *Culex quinquefasciatus* Say Infected with *Culex* Flavivirus Izabal. *PLoS Neglected Tropical Diseases*, **4**(5), e671. https://doi.org/10.1371/journal.pntd.0000671
- Krause, P. J., Telford, S. R., III, Spielman, A., Sikand, V., Ryan, R., Christianson, D., Burke, G., Brassard, P., Pollack, R., Peck, J., & Persing, D. H. (1996). Concurrent Lyme Disease and Babesiosis: Evidence for Increased Severity and Duration of Illness. *JAMA*, **275**(21), 1657–1660. https://doi.org/10.1001/jama.1996.03530450047031

Labuda, M., Nuttall, P. A., Kožuch, O., Elečková, E., Williams, T., Žuffová, E., & Sabó, A. (1993). Non-viraemic transmission of tick-borne encephalitis virus: A mechanism for arbovirus survival in nature. *Experientia*, **49**(9), 802–805. https://doi.org/10.1007/BF01923553

- Lim, J. K., & Murphy, P. M. (2011). Chemokine control of West Nile virus infection. *Experimental Cell Research*, **317**(5), 569–574. https://doi.org/10.1016/j.yexcr.2011.01.009
- Livak, K. J., & Schmittgen, T. D. (2001). Analysis of Relative Gene Expression Data Using Real-Time Quantitative PCR and the 2-ΔΔCT Method. *Methods*, **25**(4), 402–408. https://doi.org/10.1006/meth.2001.1262
- Logina, I., Krumina, A., Karelis, G., Elsone, L., Viksna, L., Rozentale, B., & Donaghy, M. (2006). Clinical features of double infection with tick-borne encephalitis and Lyme borreliosis transmitted by tick bite. *Journal of Neurology, Neurosurgery and Psychiatry*, **77**(12), 1350–1353. https://doi.org/10.1136/jnnp.2004.060731
- Marle G., Henry S., Todoruk T., Sullivan A., Silva C., Rourke S.B., Holden J., McArthur J.C., Gill M.J., Power C. Human immunodeficiency virus type 1 Nef protein mediates neural cell death: a neurotoxic role for IP-10. Virology. 2004 Nov 24;**329**(2):302-18. doi: 10.1016/j.virol.2004.08.024.
- Michelet, L., Delannoy, S., Devillers, E., Umhang, G., Aspan, A., Juremalm, M., Chirico, J., van der Wal, F. J., Sprong, H., Boye Pihl, T. P., Klitgaard, K., Bødker, R., Fach, P., & Moutailler, S. (2014). High-throughput screening of tick-borne pathogens in Europe. *Frontiers in Cellular and Infection Microbiology*, **4**, 103. https://doi.org/10.3389/fcimb.2014.00103
- Migné, C. V., Hönig, V., Bonnet, S. I., Palus, M., Rakotobe, S., Galon, C., Heckmann, A., Vyletova, E., Devillers, E., Attoui, H., Ruzek, D., & Moutailler, S. (2022). Evaluation of two artificial infection methods of live ticks as tools for studying interactions between tick-borne viruses and their tick vectors. *Scientific Reports*, **12**(1), 491. https://doi.org/10.1038/s41598-021-04498-9
- Moniuszko, A., Dunaj, J., Świ\c ecicka, I., Zambrowski, G., Chmielewska-Badora, J., \.Zukiewicz-Sobczak, W., Zajkowska, J., Czupryna, P., Kondrusik, M., Grygorczuk, S., Swierzbinska, R., & Pancewicz, S. (2014). Co-infections with Borrelia species, Anaplasma phagocytophilum and Babesia spp. In patients with tick-borne encephalitis. European Journal of Clinical Microbiology & Infectious Diseases: Official Publication of the European Society of Clinical Microbiology, 33(10), 1835–1841. https://doi.org/10.1007/S10096-014-2134-7
- Moro, M. H., Zegarra-Moro, O. L., Bjornsson, J., Hofmeister, E. K., Bruinsma, E., Germer, J. J., & Persing, D. H. (2002). Increased Arthritis Severity in Mice Coinfected with *Borrelia burgdorferi* and *Babesia microti*. *The Journal of Infectious Diseases*, **186**(3), 428–431. https://doi.org/10.1086/341452
- Muturi, E. J., & Bara, J. (2015). Sindbis virus interferes with dengue 4 virus replication and its potential transmission by *Aedes albopictus*. *Parasites and Vectors*, *8*(1), 1–10. https://doi.org/10.1186/s13071-015-0667-y
- Oechslin, C. P., Heutschi, D., Lenz, N., Tischhauser, W., Péter, O., Rais, O., Beuret, C. M., Leib, S. L., Bankoul, S., & Ackermann-Gäumann, R. (2017). Prevalence of tick-borne pathogens in questing *Ixodes ricinus* ticks in urban and suburban areas of Switzerland. *Parasites & Vectors*, **10**, 558. https://doi.org/10.1186/s13071-017-2500-2
- Ostapchuk, Y. O., Dmitrovskiy, A. M., Pak, E. A., & Perfilyeva, Y. V. (2023). A Case of Combined Infection with Tick-Borne Encephalitis and Lyme Borreliosis with Severe Meningoencephalitis and Complete Recovery. *Journal of Global Infectious Diseases*, **15**(2), 81–83. https://doi.org/10.4103/jqid.jqid 76 22
- Palus, M., Vojtíšková, J., Salát, J., Kopecký, J., Grubhoffer, L., Lipoldová, M., Demant, P., & Růžek, D. (2013). Mice with different susceptibility to tick-borne encephalitis virus infection show selective neutralizing antibody response and inflammatory reaction in the central nervous system. *Journal of Neuroinflammation*, **10**, 77. https://doi.org/10.1186/1742-2094-10-77
- Passeron, T., Lebwohl, M., Lynde, C., Alam, M. S., Laquer, V. T., Beecker, J., Ganesan, A. K., Volkova, A., Soltanalizadeh, B., Kornacki, D., & Smith, S. H. (2024). 624—Vitiligo biomarker CXCL10 correlates with clinical response in the phase 2 randomized, double-blind, vehicle-

controlled TRuE-V mechanism of action study. British Journal of Dermatology, **191**, Issue Supplement_2, Ijae266.008. https://doi.org/10.1093/bjd/ljae266.008

- Pesko K, Mores CN. Effect of sequential exposure on infection and dissemination rates for West Nile and St. Louis encephalitis viruses in *Culex quinquefasciatus*. Vector Borne Zoonotic Dis. 2009 Jun;**9**(3):281-6. doi: 10.1089/vbz.2007.0281.
- Pícha, D., Moravcová, L., & Smíšková, D. (2016). Prospective study on the chemokine CXCL13 in neuroborreliosis and other aseptic neuroinfections. *Journal of the Neurological Sciences*, **368**, 214–220. https://doi.org/10.1016/j.jns.2016.05.059
- Pietikäinen, A., Maksimow, M., Kauko, T., Hurme, S., Salmi, M., & Hytönen, J. (2016). Cerebrospinal fluid cytokines in Lyme neuroborreliosis. *Journal of Neuroinflammation*, **13**(1), 1–10. https://doi.org/10.1186/S12974-016-0745-X
- Pokorna Formanova, P., Palus, M., Salat, J., Hönig, V., Stefanik, M., Svoboda, P., & Ruzek, D. (2019). Changes in cytokine and chemokine profiles in mouse serum and brain, and in human neural cells, upon tick-borne encephalitis virus infection. *Journal of Neuroinflammation*, **16**(1), 1–14. https://doi.org/10.1186/S12974-019-1596-Z
- Porcelli, S., Deshuillers, P. L., Moutailler, S., & Lagrée, A.-C. (2024a). Meta-analysis of tick-borne and other pathogens: Co-infection or co-detection? That is the question. *Current Research in Parasitology & Vector-Borne Diseases*, **6**, 100219. https://doi.org/10.1016/j.crpvbd.2024.100219
- Porcelli, S., Heckmann, A., Deshuillers, P. L., Wu-Chuang, A., Galon, C., Mateos-Hernandez, L., Rakotobe, S., Canini, L., Rego, R. O. M., Simo, L., Lagrée, A.-C., Cabezas-Cruz, A., & Moutailler, S. (2024b). Co-infection dynamics of *B. afzelii* and TBEV in C3H mice: Insights and implications for future research. *Infection and Immunity*, **92**(8), e00249-24. https://doi.org/10.1128/iai.00249-24
- Porcelli, S., Heckmann, A., Lagrée, A.-C., Galon, C., Moutailler, S., & Deshuillers, P. (2023). Exploring the Susceptibility of C3H Mice to Tick-Borne Encephalitis Virus Infection: Implications for Co-Infection Models and Understanding of the Disease. *Viruses*, **15**(11), 2270. https://doi.org/10.3390/v15112270
- Porcelli, S., Le Roux, D., Karadjian, G., Simo, L., Mateos-Hernández, L., Galon, C., Cabezas-Cruz, A., Heckmann, A., Lagrée, A.-C., & Moutailler, S. (2025). Interaction dynamics of *B. afzelii* and TBEV in C3H mice: insights into immune response. Zenodo. https://doi.org/10.5281/zenodo.16568808
- Pospisilova, T., Urbanova, V., Hes, O., Kopacek, P., Hajdusek, O., & Sima, R. (2019). Tracking of *Borrelia afzelii* Transmission from Infected *Ixodes ricinus* Nymphs to Mice. *Infection and Immunity*, **87**(6), 10.1128/iai.00896-18. https://doi.org/10.1128/iai.00896-18
- Prandovszky, E., Horváth, S., Gellért, L., Kovács, S. K., Janka, Z., Toldi, J., Shukla, D., & Vályi-Nagy, T. (2008). Nectin-1 (HveC) is expressed at high levels in neural subtypes that regulate radial migration of cortical and cerebellar neurons of the developing human and murine brain. *Journal of NeuroVirology*, **14**(2), 164–172. https://doi.org/10.1080/13550280801898672
- Rincón, M., Anguita, J., Nakamura, T., Fikrig, E., & Flavell, R. A. (1997). Interleukin (IL)-6 Directs the Differentiation of IL-4–producing CD4+ T Cells. *The Journal of Experimental Medicine*, 185(3), 461–470. https://doi.org/10.1084/jem.185.3.461
- Rocha, S. C., Velásquez, C. V., Aquib, A., Al-Nazal, A., & Parveen, N. (2022). Transmission Cycle of Tick-Borne Infections and Co-Infections, Animal Models and Diseases. *Pathogens*, **11**(11), 1309. https://doi.org/10.3390/pathogens11111309
- Rupprecht, T. A., Koedel, U., Fingerle, V., & Pfister, H. W. (2008). The pathogenesis of lyme neuroborreliosis: From infection to inflammation. *Molecular Medicine*, **14**(3–4), 205–212. https://doi.org/10.2119/2007-00091.RUPPRECHT
- Růžek, D., Salát, J., Singh, S. K., & Kopecký, J. (2011). Breakdown of the Blood-Brain Barrier during Tick-Borne Encephalitis in Mice Is Not Dependent on CD8+ T-Cells. *PLoS ONE*, 6(5), e20472. https://doi.org/10.1371/journal.pone.0020472

Sasseville, V. G., Smith, M. M., Mackay, C. R., Pauley, D. R., Mansfield, K. G., Ringler, D. J., & Lackner, A. A. (1996). Chemokine expression in simian immunodeficiency virus-induced AIDS encephalitis. *American Journal of Pathology*, **149**(5), 1459–1467.

- Shirato, K., Kimura, T., Mizutani, T., Kariwa, H., & Takashima, I. (2004). Different chemokine expression in lethal and non-lethal murine West Nile virus infection. *Journal of Medical Virology*, **74**(3), 507–513. https://doi.org/10.1002/jmv.20205
- Shrestha, B., Samuel, M. A., & Diamond, M. S. (2006). CD8+ T Cells Require Perforin To Clear West Nile Virus from Infected Neurons. Journal of Virology, 80(1), 119. https://doi.org/10.1128/jvi.80.1.119-129.2006
- Sui, Y., Stehno-Bittel, L., Li, S., Loganathan, R., Dhillon, N. K., Pinson, D., Nath, A., Kolson, D., Narayan, O., & Buch, S. (2006). CXCL10-induced cell death in neurons: Role of calcium dysregulation. European Journal of Neuroscience, **23**(4), 957–964. https://doi.org/10.1111/j.1460-9568.2006.04631.x
- Štěpánová-Tresová, G., Kopecký, J., & Kuthejlová, M. (2000). Identification of *Borrelia burgdorferi* sensu stricto, *Borrelia garinii* and *Borrelia afzelii* in *Ixodes ricinus* Ticks from Southern Bohemia Using Monoclonal Antibodies. *Zentralblatt Für Bakteriologie*, **289**(8), 797–806. https://doi.org/10.1016/S0934-8840(00)80005-5
- Thomas, V., Anguita, J., Barthold, S. W., & Fikrig, E. (2001). Coinfection with Borrelia burgdorferi and the Agent of Human Granulocytic Ehrlichiosis Alters Murine Immune Responses, Pathogen Burden, and Severity of Lyme Arthritis. Infection and Immunity, **69**(5), 3359–3371. https://doi.org/10.1128/IAI.69.5.3359-3371.2001
- Waiß, C., Ströbele, B., Graichen, U., Klee, S., Gartlehner, J., Sonntagbauer, E., Hirschbichler, S., Tinchon, A., Kacar, E., Wuchty, B., Novotna, B., Kühn, Z., Sellner, J., Struhal, W., Bancher, C., Schnider, P., Asenbaum-Nan, S., & Oberndorfer, S. (2024). CXCL13 as a biomarker in the diagnostics of European lyme Neuroborreliosis—A prospective multicentre study in Austria. Journal of Central Nervous System Disease, 16, 11795735241247026. https://doi.org/10.1177/11795735241247026
- Wallner, G., Mandl, C. W., Ecker, M., Holzmann, H., Stiasny, K., Kunz, C., & Heinz, F. X. (1996). Characterization and complete genome sequences of high- and low-virulence variants of tick-borne encephalitis virus. Journal of General Virology, 77(5), 1035–1042. https://doi.org/10.1099/0022-1317-77-5-1035
- Wormser, G. P., McKenna, D., Scavarda, C., Cooper, D., El Khoury, M. Y., Nowakowski, J., Sudhindra, P., Ladenheim, A., Wang, G., Karmen, C. L., Demarest, V., Dupuis, A. P., & Wong, S. J. (2019). Co-infections in persons with early lyme disease, New York, USA. *Emerging Infectious Diseases*, 25(4), 748–752. https://doi.org/10.3201/eid2504.181509
- Wu-Chuang, A., Mateos-Hernandez, L., Maitre, A., Rego, R. O. M., Šíma, R., Porcelli, S., Rakotobe, S., Foucault-Simonin, A., Moutailler, S., Palinauskas, V., Aželytė, J., Sĭmo, L., Obregon, D., & Cabezas-Cruz, A. (2023). Microbiota perturbation by anti-microbiota vaccine reduces the colonization of *Borrelia afzelii* in *Ixodes ricinus*. *Microbiome*, **11**(1), 151. https://doi.org/10.1186/s40168-023-01599-7
- Yasumura, Y., & Kawakita, Y. (1963). Studies on SV40 in tissue culture-preliminary step for cancer research in vitro. Nihon Rinsho, 21, 1201–1219.
- Zeidner, N., Mbow, M. L., Dolan, M., Massung, R., Baca, E., & Piesman, J. (1997). Effects of *Ixodes scapularis* and *Borrelia burgdorferi* on modulation of the host immune response: Induction of a TH2 cytokine response in Lyme disease-susceptible (C3H/HeJ) mice but not in disease-resistant (BALB/c) mice. Infection and Immunity, **65**(8), 3100–3106. https://doi.org/10.1128/iai.65.8.3100-3106.1997
- Zeidner, N. S., Dolan, M. C., Massung, R., Piesman, J., & Fish, D. (2000). Coinfection with *Borrelia burgdorferi* and the agent of human granulocytic ehrlichiosis suppresses IL-2 and IFNγ production and promotes an IL-4 response in C3H/HeJ mice. *Parasite Immunology*, **22**(11), 581–588. https://doi.org/10.1046/J.1365-3024.2000.00339.X
- Zhang, B., Chan, Y. K., Lu, B., Diamond, M. S., & Klein, R. S. (2008). CXCR3 Mediates Region-Specific Antiviral T Cell Trafficking within the Central Nervous System during West Nile Virus

- Encephalitis. *The Journal of Immunology*, **180**(4), 2641–2649. https://doi.org/10.4049/JIMMUNOL.180.4.2641
- Zhang, X., Zheng, Z., Liu, X., Shu, B., Mao, P., Bai, B., Hu, Q., Luo, M., Ma, X., Cui, Z., & Wang, H. (2016). Tick-borne encephalitis virus induces chemokine RANTES expression via activation of IRF-3 pathway. *Journal of Neuroinflammation*, **13**(1), 1–18. https://doi.org/10.1186/s12974-016-0665-9
- Zheng, W. Q., Xuan, X. N., Fu, R. L., Tao, H. Y., Liu, Y. Q., Liu, X. Q., Li, D. M., Ma, H. M., & Chen, H. Y. (2018). Tick-Borne Pathogens in Ixodid Ticks from Poyang Lake Region, Southeastern China. *The Korean Journal of Parasitology*, **56**(6), 589–596. https://doi.org/10.3347/KJP.2018.56.6.589
- Zou, Y., Huang, F., Sun, J., Zheng, Y., Dai, G., Wang, T., Zhu, C., Yan, Y., Wang, R., & Chen, Z. (2025). The role of IFN-γ/CXCL10 axis in *Mycoplasma pneumonia* infection. *Scientific Reports*, **15**, 2671. https://doi.org/10.1038/s41598-024-84969-x